

Transcriptomic and Metabolomics Analyses Show that High Carbohydrate Induces Fatty Liver in Blunt Snout Bream (*Megalobrama amblycephala*)

Wassana Prisingkorn, Panita Prathomya, Han Liu, Fang-Yu Deng, Yu-Hua Zhao * and Wei-Min Wang *

College of Fisheries Huazhong Agricultural University, Key Lab of Freshwater Animal Breeding, Ministry of Agriculture, Key Lab of Agricultural Animal Genetics, Breeding and Reproduction of Ministry of Education, Freshwater Aquaculture Collaborative Innovation Center of Hubei Province, Wuhan 430070, China;

wp_abrc@yahoo.com (W.P.); p_prathomya@yahoo.com (P.P.); liuhan@mail.hzau.edu.cn (H.L.)

* Correspondence: zhaoyuhua2005@mail.hzau.edu.cn (Y.-H.Z.); wangwm@mail.hzau.edu.cn (W.-M.W.)

Abstract

A high intake of carbohydrates, associated with obesity, is one of the major causes of fatty liver disease in humans. This study investigated how high carbohydrate intake induces fatty liver disease in Blunt snout bream (*Megalobrama amblycephala*). Blunt snout bream were fed a high-carbohydrate diet (HCBD) for 60 days. Their growth indices were evaluated, and the transcriptomes, metabolites, biochemistry, and histology of their blood and livers were analyzed. The final weight, weight gain, specific growth rate, and feed conversion ratio were all higher in the HCBD group than in the control group, but not significantly so ($P > 0.05$). The hepatosomatic index (HSI) differed significantly in the two groups ($P < 0.05$), and the metabolomics results showed that a high carbohydrate intake induced significant increases in plasma α/β -glucose, succinate, and tyrosine, which could increase hepatic glycogen and triglyceride. Low levels of betaine were also found in the livers of the HCBD group. The histology and blood biochemistry results suggested abnormal liver, with excessive lipid accumulation and liver damage. A transcriptome analysis and quantitative reverse transcription-PCR (RT-qPCR) indicated that the expression of the factors INSR, IRS, PI3K, PDK, AKT, ACC, IL6, AP1, ChREBP-MLX, PEPCK, and FBP in the insulin signaling pathway was significantly upregulated and that of SOCS3, GSK3 β , and AMPK significantly downregulated in the HCBD. This pattern is associated with the nonalcoholic fatty liver disease (NAFLD) pathway. This study extends our understanding of how high carbohydrate causes increased fat deposition in the liver, enhanced glycolysis (α/β -glucose) in the plasma, and reduced betaine in the liver. This leads to activation of hepatocyte insulin resistance and lipogenesis by regulating the expression of genes related to fatty liver disease.

Keyword: blunt snout bream; high carbohydrate; transcriptome; metabolomics; insulin resistance; fatty liver disease

Introduction

Carbohydrates are one of the main sources of energy in most animal diets, and the liver is the major site of carbohydrate metabolism and triglyceride synthesis. Glucose and other simple sugars obtained from the digestion of dietary starches and polysaccharides (carbohydrates) are metabolized by the liver to provide substrates, such as acetyl-CoA, for the synthesis of fatty acids and numerous other molecules. Carbohydrate is usually the cheapest dietary energy supplying nutrient, and its appropriate introduction may reduce catabolism of protein and lipid for energy. This may lead to a reduction of formulated diets cost and ammonia excretion by amino acid metabolism [1]. Inclusion of carbohydrate in the diet of several fish species appears to produce positive effects on growth and digestibility [2–4]. The ability of fish to use dietary carbohydrates varies widely among and within species and is closely associated with their feeding habits. Fish generally have high dietary protein requirements and are considered to be poor utilizers of dietary carbohydrates [5–8]. If the appropriate levels of carbohydrates are not available, however, there may be negative effects on the nutrient utilization, growth, metabolism, and health of the fish [9,10]. Compared with mammals, the utilization of carbohydrate in fish is limited and can be affected by the level and source of the dietary carbohydrate. For example, reduced growth performance and feed utilization were observed in several fish species fed a glucose diet compared with those of fish fed a starch diet [11,12]. Over-ingestion of simple carbohydrates, such as sucrose and fructose is a major cause of nonalcoholic fatty liver disease (NAFLD) [13]. Although a high intake of carbohydrates has been associated with increased risks of fatter fish (obesity) and NAFLD, the available data are often ambiguous [14,15]. Therefore, several fish have been used to investigate whether fish livers are affected by excessive carbohydrate, including changes in liver size, cellular architecture, gene expression patterns, and lipid accumulation [16,17].

The blunt snout bream, *Megalobrama amblycephala*, is an herbivorous freshwater fish that is native to China and has a low carbohydrate tolerance. In recent years, the need to maximize the use of dietary nonprotein energy sources [18,19] has inevitably resulted in the severe deposition of body lipids in fish, coupled to increasing outbreaks of fatty liver diseases. However, there has been no report of fatty liver disease in this species until now. There are also few reports of the effects of a high-carbohydrate diet (HCBD) on the lipid metabolism of the blunt snout bream, which is a cause of obesity-associated NAFLD.

Therefore, to understand better the mechanism of NAFLD and to advance the aquaculture of the blunt snout bream, we investigated how a high carbohydrate intake induces fatty liver disease in this fish model based on transcriptomic and metabolomics analyses. We examined the effects of HCBD on the hepatic transcriptome, hepatic and serum metabolomics, blood biochemistry, growth indices, and liver histology.

Results

High carbohydrate induced body and histology changes

The bodyweights, food utilization, and biometric parameters of blunt snout bream fed a normal diet (control) or HCBD are shown in Table 2. After the 60-day feeding period, the survival rate of all fish was > 94% and did not differ statistically ($P > 0.05$) between the groups. The final weight, weight gain, SGR, and FCR were all higher in the HCBD group than in the control group, but did not differ significantly ($P < 0.05$; Table 2). However, HSI was significantly higher in the HCBD group than in the control group ($P < 0.05$; Table 2).

The liver histology was consistent with the HSI. The control group showed regular hepatocytes with large and spherical nuclei centrally located in moderate cytoplasm and a small number of lipid droplets (Figure 1A). In contrast, the liver histology of the HCBD group showed swollen hepatocytes with large diffuse lipid vacuoles, abnormal endothelial cells in the central vein, inflammatory infiltration, and some hypertrophy of the hepatocytes (Figure 1B). Thus, fatty liver was apparent in the HCBD group.

High carbohydrate induced changes in serum biochemistry

The HCBD induced changes in the fish's serum biochemistry, affecting ALT, AST, TG and LDL. ALT and AST were both significantly elevated in the HCBD group compared with the control group ($P < 0.05$), whereas TG was significantly reduced ($P < 0.05$) (Figure 2). Serum LDL was significantly higher in the HCBD group than in the control group ($P < 0.05$; Figure 2).

High carbohydrate induced metabolomic changes in the serum and liver

The metabolomic analysis results for the blood sera and livers of the control and HCBD groups, inferred from ¹H-NMR metabolite profiles, are shown in Figure 3. The NMR spectra of the sera indicated differences in α/β -glucose (glycolysis metabolic pathway), and succinate and tyrosine (tricarboxylic acid [TCA] cycle metabolic pathway) (Table S2). The relative contents of various metabolites, including α -glucose ($P < 0.01$), β -glucose ($P < 0.05$), succinate ($P < 0.05$), and tyrosine ($P < 0.01$), were significantly elevated in the HCBD group (Figure 3A). The NMR spectra specifically showed that betaine was very significantly reduced in the livers of the HCBD group compared with the control group ($P < 0.01$; Figure 3B, Figure S1 and 2, Table S2).

High carbohydrate induced transcriptomic changes in the liver

Nonnormalized cDNA libraries were constructed from six tissue samples and Solexa/Illumina paired-end sequencing yielded 157,063 transcripts and 96,427 unigenes from the three libraries. After stringent quality assessment and data filtering, 22,415,280 control and 19,837,027 HCBD high-quality reads were selected for

further analysis. The GC contents of the control and HCBD were 47.76% and 47.80%, respectively (with an average length of Q30 base percentage 80.01 per group).

The functions of the unigene sequences of the control and HCBD groups were predicted and classified by searching the Clusters of Orthologous Groups (COG) database, which cataloged the sequences into 24 categories (Figure 4A). The major group was 'general function prediction only' (412 genes; 15.92%), followed by 'translation, ribosomal structure, and biogenesis' (348 genes; 13.45%) and 'posttranslational modification, protein turnover, chaperones' (227 genes; 8.77%). Only three unigenes were allocated to 'cell mobility' in the HCBD group. No unigenes were related to 'extracellular structures' or 'nuclear structure' (Figure 4A).

The three main categories of GO annotations were 'biological processes' (14,583, 35.78%), 'cellular components' (11,271, 27.66%), and 'molecular function' (14,901, 36.56%) (Figure 4B). For biological processes, the most frequent GO terms were 'cellular process', 'metabolic process', and 'single-organism process'. For cellular components, genes involved in 'cell part', 'macromolecular complex', and 'organelle' were most strongly represented. In the category of molecular function, the term 'binding' accounted for the highest proportion of annotations, followed by 'catalytic activity' and 'structural molecule activity'. Differentially expressed genes (DEGs) were identified by the pairwise comparison of the control and HCBD genes, and 5,556 genes were significantly differentially expressed between the control and HCBD fish, with 1,318 upregulated and 4,238 downregulated (Figure 4C). To further clarify the biological pathways affected by the HCBD in the blunt snout bream, the unigene sequences were mapped with the KEGG Pathway tools. This process compared the control and HCBD groups and assigned 1,895 unigenes to a total of 319 pathways. In these predicted pathways, involving six KEGG categories (Figure 4D), the most strongly represented functional category was 'human disease', containing 709 unigenes, including 96 unigenes involved in NAFLD. The least strongly represented functional category was 'cellular process', with 412 unigenes. Interestingly, several pathways associated with metabolic pathways were identified in the database. 109 of metabolisms were linked to 'metabolic processes. Further information on the predicted pathways may be useful in investigating the functions of the genes affected by HCBD in the blunt snout bream. The transcriptomic profiles showed that HCBD played an active role in the NAFLD pathway and the insulin signaling pathway, which may lead to the development of fatty liver diseases, including hepatocyte insulin resistance (Table 3).

Comparisons of the hepatic transcriptomes and RT-qPCR results for the control and HCBD groups showed that the expression of some genes involved in the NAFLD pathway, according to the results of KEGG pathway analysis, was significantly altered. For example, the expression of suppressor of cytokine signaling 3 (SOCS3) was

downregulated ($P < 0.05$), which caused the expression of the insulin receptor (INSR) and the insulin receptor substrate (IRS) to be upregulated ($P < 0.01$), which further led to the upregulation of phosphoinositide-3-kinase (PI3K), phosphoinositide-dependent protein kinase 1 (PDK1), and RAC-gamma serine/threonine-protein kinase (AKT). Glycogen synthase kinase 3 beta (GSK3 β) was inactivated because its expression correlates negatively with AKT, and glycogen (starch) synthase (GYS) was increased with the reduction in GSK3 β . Thus, the synthesis of glycogen was increased. After the ingestion of HCBD, the fish reacted with prolonged postprandial hyperglycemia. Therefore, various hypotheses can explain the poor utilization of dietary carbohydrate by fish. Insulin resistance was also observed, which is one of the causes of fatty liver disease (Figure 5, 6).

The expression of acetyl-CoA carboxylase (ACC) was also significantly upregulated by the reduction in AMP-activated protein kinase (AMPK) (Figure 5, 6). Therefore, lipogenesis increased. If lipogenesis increases beyond normal levels, then TG accumulates in the liver, which contributes to fatty liver disease.

The regulation of the expression of the fructose-1,6-bisphosphatase 1 (FBP) gene was also altered, which is related to the dysregulation of carbohydrate transport and metabolism. The expression of interleukin 6 (IL6), transcription factor AP-1 (AP1), phosphoenolpyruvate carboxykinase (PEPCK), and MAX-like protein X (MLX, ChREBP) was upregulated, and all these genes are associated with the NAFLD pathway (Figure 5 and Table 3).

Discussion

The growth performance results showed that high carbohydrate had positively affected on body weight, growth rate and utilization rate of food, but it was not significantly different compared to control. This was similar to the previous studies in rainbow trout (*Oncorhynchus mykiss*) [20], Indian major carp (*Cirrhinus mrigala*) [21] and gilthead sea bream (*Sparus aurata*) [22]. These references reported that high carbohydrate had no significant effect on growth performances. In contrast, other research reported that excessive carbohydrate levels had effect on growth performances by reducing the growth rate, and increasing FCR in blunt snout bream [23] and grass carp (*Ctenopharyngodon idellus*) [24]. The reason of difference from our result may be related to the different carbohydrate content in different diets.

HCBD also affected the liver. HSI was significantly higher in the HCBD group than in the control (Table 2). Similarly, increasing levels of carbohydrate affected the HSI of the gilthead sea bream (*Sparus aurata*) [22]. Interestingly, the increase in the HSI when fish were fed HCBDs may be related to an increase in glycogen deposition in the fish liver [25–27]. A previous study also showed that the blunt snout breams fed HCBD had a significantly higher hepatic glycogen content than those fed the control diet [28]. This result is also consistent with

our metabolite results, which showed that a high carbohydrate intake induced significant increases in plasma α/β -glucose, succinate, and tyrosine (Figure 2). Because α/β -glucose can be converted to glycerin or glycogen in the glycolysis/gluconeogenesis pathway and succinate and tyrosine can be converted to acetyl-CoA in the TCA cycle pathway, these increases in plasma α/β -glucose, succinate, and tyrosine could lead to increases in hepatic glycogen. Thus, the HSI of the HCBD group increased with increased glycogen deposition in the fish liver. Insulin resistance accompanied this accumulation of hepatic glycogen [29-32] and insulin resistance is one cause of fatty liver disease. Therefore, a high carbohydrate intake induces the increase in HSI and a high HSI is bad for the hepatic health of fish.

Pathological liver damage was also observed in the HCBD group. This is consistent with previous studies that reported abnormal hepatocytes when the carbohydrate levels were increased in the diet of the blunt snout bream [28], juvenile yellow catfish (*Pelteobagrus fulvidraco*) [33], *Labeo rohita* juveniles [34], and *L. rohita* fry [35]. The lipid vacuolization of hepatocytes indicated an accumulation of fat in the liver. Both fat accumulation and inflammatory infiltration are precursors of fatty liver disease. From These results showed that high-carbohydrate diets can increase bodyweight (obesity), HSI, glycogen, and fat accumulation in the liver. Obesity and glycogen accumulation can cause insulin resistance, which contributes to fatty liver. HSI correlates negatively with hepatic health in fish. Therefore, HCBDs are associated with fatty liver diseases caused by fat and glycogen accumulation in the liver, increased bodyweight, and high HSI.

The serum biochemistry showed high ALT and AST levels are indicators of liver damage and are associated with NAFLD and NASH [36,37]. In this study, the ALT and AST levels were significantly higher in the HCBD group than in the control group, indicating that a high carbohydrate intake can cause unhealthy livers, with NAFLD or NASH. This is consistent with our results for liver histology, serum metabolomics, and HSI, which are all related to fatty liver disease.

Higher levels of LDL was observed in the HCBD group than in the control group. This is consistent with previous research that reported higher concentrations of LDL in obese rats than in lean rats [38] and with our results (bodyweight was higher in the HCBD group). These high LDL levels may arise because high carbohydrate causes more cholesterol to be synthesized in the liver, and more LDL is then required to transport this cholesterol to other peripheral tissues. LDL is also one of the causes of hepatic inflammation and plays a critical role in the development of NAFLD [39]. Therefore, this high level of LDL is also consistent with our histological results in the liver, which indicated excessive lipid accumulation and liver damage.

Although a lot of lipid accumulated in the liver, serum TG was reduced in the HCBd group. Liver dysfunction (attributable to liver damage and fatty liver) may explain this phenomenon, insofar as the damaged liver cannot transport TG to the blood or other peripheral tissues.

The lower serum TG in the HCBd group is also consistent with the results of the metabolomics analysis of the liver in that betaine was significantly reduced in the HCBd group. It had been reported that a decline in betaine indicates lower serum TG in the diabetic *db/db* mouse model [30]. Betaine is the product of the irreversible oxidation of choline in the liver and kidney. It can effectively prevent fructose-induced NAFLD and improve liver function by inhibiting inflammatory factors, reducing lipid peroxidation, reducing endoplasmic reticulum stress, and preventing apoptosis [40-42]. This indicates that a decline in liver betaine is a consequence of the pathological changes associated with a high carbohydrate intake. In this study, betaine was reduced by the intake of excess carbohydrate, which contributed to the formation of fatty liver. This is consistent with the histopathological and serum biochemical analyses.

In the transcriptome results we found that SOCS3 in the NAFLD pathway was downregulated in the HCBd group (Figure 5), which induced increases in INSR and IRS (Figure 5) because SOCS3 correlates negatively with INSR and IRS, and plays an important role in the pathogenesis of obesity in animal models [43]. INSR is a member of the receptor tyrosine kinase family, and binds insulin and other ligands that regulate glucose uptake and release and the synthesis and storage of carbohydrates, lipids, and protein [44]. Insulin may also regulate its own expression by binding to cell-surface INSR and stimulating a phosphorylation-dependent signaling cascade [45]. IRS stimulates PI3K expression, which was significantly upregulated in the HCBd group (Figure 5), and the generation of phosphatidylinositol-(3,4,5)-triphosphate (PIP3), a lipid second messenger that activates several PIP3-dependent serine/threonine kinases, including PDK1 and subsequently AKT/PKB [44]. This is consistent with our study and with the known functions of this protein in insulin signaling [46]. 3-Phosphoinositide-dependent protein kinase 1 (PDK1/2, PDK1) was significantly upregulated in the HCBd group (Figure 5), so its expression is responsive to the consumption of carbohydrate. PDK1 is a master kinase activated by several growth factors and hormones, and plays an important role in various signaling pathways, including insulin signaling. A genetic analysis of the PDOK1 signaling pathway in *Drosophila melanogaster* and mice suggested that this pathway plays an important role in regulating organism size [47]. Normally, AKT is phosphorylated by PDK1. The increase in AKT/PKB appeared to inhibit GSK3 β expression, which was significantly downregulated (Figure 5), but not through mTOR. The phosphorylation of GYS by GSK3 inhibits glycogen synthesis (Figure 5). GYS, an enzyme that catalyzes the final step and is the limiting enzyme in glycogen synthesis, is a major substrate of GSK3 [48].

The inactivation of GSK3 by AKT promotes glucose storage as glycogen. By promoting glucose storage, insulin inhibits the production and release of glucose in the liver by blocking gluconeogenesis and glycogenolysis [49]. In human research, Hazlehurst reported that insulin resistance in adipose tissue remains an important component of the pathogenesis of NAFLD, leading to increases in circulating glucose and the availability of lipid substrates for the accumulation of hepatic lipids [50].

AMP-activated protein kinase (AMPK) regulates insulin sensitivity. A continuous reduction in AMPK activity (Figure 5), is accompanied by insulin resistance, whereas AMPK activation increases insulin sensitivity. AMPK phosphorylation activates fatty acid synthesis by inhibiting ACC gene expression. In this study, ACC gene expression was upregulated by the inactivation of AMPK (Figure 5). Similarly, AMPK activity decreased when hepatocytes were exposed to high glucose. Exposing cells to high glucose concentrations induces a model of insulin resistance in which AMPK is inhibited and lipids accumulate [51]. AMPK also controls key players in various metabolic pathways and is therefore a major regulator of glucose and lipid metabolism, with many important roles in tissues [52]. The reduction in AMPK is consistent with the increase in *de novo* lipogenesis in NAFLD [53-55].

According to our metabolomics data, a significant reduction in liver betaine was observed in the HCBD group. This is consistent with the transcriptomic results. A previous study showed that betaine can prevent high-fructose-intake-induced NAFLD by suppressing high-fructose-induced gluconeogenesis by moderating (upregulating) the expression of the AKT/PKB gene [29]. Our transcriptomic analysis showed that HCBD was associated with the upregulation of AKT/PKB and the downregulation of AMPK (Table 3). Another report suggested that betaine directly affects hepatocytes by increasing the tyrosine phosphorylation of IRS1, thus affecting PI3K and activating AKT/PKB [31].

Hepatic IL6 was also upregulated in the HCBD group (Figure 5). IL6 is an important proinflammatory adipocytokine that is always significantly elevated in the fat cells of obese and insulin-resistant individuals and NAFLD patients, and is clearly evident in adipose cells on liver histology [56-58]. ChREBP-MLX was also upregulated in the HCBD group, and the encoded protein causes *de novo* fatty acid synthesis. Recently, many researchers have reported that the liver transcription factor ChREBP-MLX is required for the induction of glycolytic gene expression by glucose [59-61]. This supports the many reports that ChREBP-MLX is always responsive to the consumption of high levels of carbohydrate [62-63]. Given the ability of ChREBP-MLX to bind and activate the transcription of several lipogenic enzyme genes, the activation of ChREBP-MLX may be the glucose-dependent mechanism responsible for the synergistic induction of fatty acid synthesis by glucose and

insulin [63]. Transcription factor activator protein 1 (AP1) was also upregulated in the HCBD group (Figure 5), and increases in AP1 transcription have been linked to obesity, hepatic lipid metabolism, and NAFLD [64]. In the HCBD group, the PEPCK gene was also upregulated (Table 3). PEPCK is a key enzyme in the synthesis of glucose in the liver and kidney, and plays a role in hepatic energy metabolism (energy production and conversion) [65,66]. FBP is carbohydrate transport and metabolism protein that acts via the insulin signaling pathway, which is associated with NAFLD. These data clearly show that the consumption of an HCBD can lead to fatty liver disease. Finally, we verified HCBD increases the accumulation of lipid in the liver, which was reflected in the liver histology, HSI, and serum biochemistry results. Disturbances in metabolic pathways were also apparent, which induced changes in the expression of genes in the NAFLD pathway, which are all associated with fatty liver disease (Figure 6).

Materials and methods

Diet preparation

Two diets (Table 1) were formulated with a protein level of 30% and total energy > 17 MJ/kg: the HCBD (> 30% carbohydrate) and the normal control diet. The diets were air-dried, sealed in airtight bags, and stored at -20°C until use.

Proximate analysis

The crude protein, crude lipid, moisture, and ash in the feeds were determined with standard methods (AOAC 1995). Moisture was determined by oven-drying at 105°C . Ash was measured using a muffle furnace at 550°C . Crude protein ($\text{N} \times 6.25$) was determined with the Kjeldahl method after acid digestion with the Kjeltex system (Kjeltex 2300 Analyzer, Foss Tecator, Hoganas, Sweden). Crude lipid was evaluated with the ether extraction method using the Soxtec System HT (Soxtec System HT6, Tecator). The energy contents of the diets were measured with bomb calorimetry using a Parr 6200 calorimeter equipped with a Parr 1108 Oxygen Bomb and a Parr 6510 water handling system (Parr Instrument Company, Moline, IL, USA).

Animal rearing and experimental procedures

Healthy juvenile blunt snout bream were obtained from a breeding center (Huazhong Agricultural University, Wuhan, China). The fish were placed in four 1000 L fiberglass tanks and fed the experimental diets for 14 days to acclimate them to the laboratory conditions at the College of Fisheries, Huazhong Agricultural University, before the start of the growth study. Fish of similar sizes (average weight, 48.13 ± 0.02 g) were randomly distributed to six fiberglass tanks at a stocking density of 45 fish/tank. The fish were fed one of the two experimental diets (the

control or HCBD, with three replicates per diet). The period of the rearing trial was 60 days. The amount of diet fed to the fish was 2.0%–4.0% of their bodyweights. Therefore, the ration size was adjusted according to the changes in the fish bodyweights in each tank. The fish were fed twice daily. Fecal matter was removed twice daily before feeding.

Sample collection

The fish were sampled on day 60. Before sampling, five fish from each tank were anesthetized with 100 mg/L tricaine methanesulfonate (MS-222; Sigma, USA) and surgically dissected. Blood serum samples were collected with the standard protocol for clinical chemistry measurements. Livers were sampled and immediately placed in liquid nitrogen for 6 h, and then the blood and liver samples were stored at -80°C until analysis. Fish weight, body length, liver weight, final number of fish, and feed consumed were determined to analyze various growth indices, such as survival, specific growth rate (SGR), feed conversion ratio (FCR), condition factor (CF), and hepatosomatic index (HSI). The data were analyzed statistically with SPSS version 11.5 (SPSS, Chicago, IL, USA). Statistical differences were determined with an unpaired two-tailed analysis (t test). Comparisons with $P \leq 0.05$ were considered statistically significant. Results were expressed as means \pm SD.

Histology

The livers of the blunt snout bream were immediately fixed in paraformaldehyde, embedded in paraffin, cut into $5\ \mu\text{m}$ sections, and stained with hematoxylin and eosin (H&E).

Metabolomics analysis

Clinical biochemistry

Serum biochemistry parameters were measured with commercial kits produced by Jiancheng Bioengineering Institute (Nanjing, China) with a Tecan analyzer (Tecan, Ltd). The parameters included alanine transaminase (ALT), aspartate transaminase (AST), triglyceride (TG) and low-density lipoprotein (LDL).

Metabolites determined with nuclear magnetic resonance (NMR) spectroscopy

Each plasma sample ($170\ \mu\text{L}$) was mixed with $340\ \mu\text{L}$ of phosphate buffer ($45\ \text{mM}$, pH 7.47, 50% D_2O) containing 0.9% NaCl in a 5 mm NMR tube and used directly for the NMR analysis. Liver tissues (about 50 mg) were homogenized in cold methanol and water (v/v 2:1) using a Qiagen TissueLyser (Retsch GmbH, Germany). All plasma NMR spectra were acquired at 298 K on a Bruker Avance III 600 MHz NMR spectrometer (600.13 MHz for ^1H frequency) equipped with a cryogenic probe (Bruker Biospin, Germany). One-dimensional ^1H NMR spectra were acquired with the Carr–Purcell–Meiboom–Gill pulse train [67]. The NMR spectroscopic analysis, NMR data processing, and multivariate data analysis were performed according to An [68].

Transcriptomic analysis

RNA extraction

The total RNA was extracted from each sample with RNAiso Plus Reagent (Takara Bio Inc., Dalian, China), according to the manufacturer's instructions. The quality of the total RNA from individual tissue samples was evaluated with electrophoresis in 1% agarose gels and the RNA was quantified spectrophotometrically with a NanoDrop 2000 spectrophotometer (Thermo Scientific, Delaware, USA) and an Agilent Bioanalyzer 2100 (Agilent, Santa Clara, CA). Equal amounts of total RNA from the liver tissues were dissolved in RNase-free water and pooled in equal quantities to generate the control and HCBD samples.

cDNA library preparation and Illumina sequencing

High-quality total RNA (5 µg, 100 ng/µL) samples were sent to the Biomarker Biotechnology Corporation (Beijing, China) for the preparation of RNA-seq libraries. All the libraries were sequenced with the Illumina HiSeq™ 2500 platform (Biomarker Technologies Corporation, Beijing, China).

De novo assembly of sequencing reads

Raw reads of the transcriptome datasets (control and HCBD) were cleaned by filtering out adaptor-only reads and low-quality reads. The adaptor-only reads (nt length of the recognized adaptor ≤ 13 and the remaining adaptor-excluded nt length ≤ 35) were filtered from the raw reads. Reads in which more than 80.01% of bases had a Q value of ≤ 30 were filtered out with the Fastq_filter software (Biomarker Technologies Co., Ltd). The clean reads were then assembled with the short-reads-assembling program Trinity, version Trinityrnaseq_r2012-06-08, with a similarity of 90%. Trinity contains three software modules, including Inchworm, Chrysalis, and Butterfly. Redundant sequences were eliminated, and the longest transcripts were recognized as unigenes, which were grouped together for the final assembly and subsequent annotation.

Annotation

Unique reads were aligned to a series of protein databases using BLASTx (E -value $\leq 10^{-5}$), including the NCBI non-redundant (NR), Swiss-Prot, TrEMBL, Kyoto Encyclopedia of Genes and Genomes (KEGG), and Gene Ontology (GO) databases. To evaluate the coverage depth, all usable reads were realigned to each unique read using HMMER and the Pfam database, and then normalized to reads per kb per million reads (RPKM) values. The difference in read abundance between the samples were then calculated based on the ratio of the RPKM values, and the false discovery rate (FDR) control method was used to identify the threshold of the P value in multiple test, in order to compute the significance of the differences in transcript abundance. Here, only unique reads with an absolute value of \log_2 ratio ≥ 1 and an FDR significance score < 0.01 were used for the subsequent analysis.

Gene expression analysis

The numbers of reads in the RNA-seq analysis were normalized to RPKM values to compute the gene expression levels. Differentially expressed genes were detected with the EBseq software (version 1.1.7) in pair-wise comparisons. A Benjamini–Hochberg FDR < 0.01 was used to correct the result for multiple testing. Genes were defined as differentially expressed when they showed parameters FDR < 0.001 and $|\log_2 \text{ratio}| > 1$ (the RPKM value of the gene in one sample was at least two-fold higher than in another sample).

RT–qPCR analysis

cDNA was prepared from the total RNA extracted from the liver samples with RNAiso Plus Reagent (Takara Bio Inc.), according to the manufacturer's instructions. The cDNA libraries were serially diluted 10-fold and used as the templates for RT–qPCR with the primers listed in Table S1. The primers were designed using the Primer Premier 5 software (Premier Biosoft, USA) [69] and synthesized by Tsingke Biological Technology (Wuhan) Co., Ltd. 18S rRNA and *Rpl13a* were used as the endogenous reference genes [70]. RT–qPCR was performed with LightCycler®480 II and SYBR® Premix Ex Taq™ (Takara Bio Inc.), according to the manufacturer's instructions. The expression levels of the target genes were normalized to the expression of 18S rRNA and *Rpl13a*, and expressed as fold changes relative to the target gene expression in the control group using the $2^{-\Delta\Delta C_t}$ method [71]. The RT–qPCR data were analyzed statistically with Microsoft Excel and with one-way analysis of variance (ANOVA) with the SPSS 16.0 software. Differences were considered statistically significant at $P < 0.05$ and $P < 0.01$.

Conclusions

The transcriptomes, metabolomics, serum biochemistry, growth indices, and histological profiles observed in this study show that HCBd can lead to increased fat deposition in the fish liver, and enhanced plasma glycolysis (α/β -glucose), and can activate insulin resistance and lipogenesis in hepatocytes through the up- or downregulation of the expression of genes related to fatty liver disease.

Acknowledgments: We would like to thank the members of College of Fisheries Huazhong Agricultural University, Key Lab of Freshwater Animal Breeding, and Ministry of Agriculture for technical help. We also wish to thank for Professor. George Britton, Dr. Ivan Jakovlic and Shaokui yi for helpful discussions. This study was supported by Natural Science Foundation of China (No. 31401976) and the earmarked fund for Modern Agro-

industry Technology Research System entitled “Staple Freshwater Fishery Industry Technology System” (No.CARS-46-05).

Author contributions : The authors’ responsibilities were as follows—WW and YZ designed the study; WP and YZ conducted research; WP, PP and YZ provided the materials; WP, PP, YZ and FD collected the data; WP, YZ and HL analyzed the data; All authors read the manuscript and provided comments and suggestions for improvements.

Conflicts of Interest: The authors declare no competing financial interests.

References

1. Enes, P.; Peres, H.; Couto, A.; Oliva-Teles, A. Growth performance and metabolic utilization of diets including starch, dextrin, maltose or glucose as carbohydrate source by gilthead sea bream (*Sparus aurata*) juveniles. *Fish Physiol. Biochem.* 2010, 36, 903–910.
2. Li, X. F.; Wang, Y.; Liu, W. B.; Jiang, G. Z.; Zhu, J. Effects of dietary carbohydrate/lipid ratios on growth performance, body composition and glucose metabolism of fingerling blunt snout bream *Megalobrama amblycephala*. *Aquac. Nutr.* 2013, 19, 701–708.
3. Hung, L. T.; Lazard, J.; Mariojouis, C.; Moreau, Y. Comparison of starch utilization in fingerlings of two Asian catfishes from the Mekong River (*Pangasius bocourti* Sauvage, 1880, *Pangasius hypophthalmus* Sauvage, 1878). *Aquac. Nutr.* 2003, 9, 215–222.
4. WATANABE, T. Strategies for further development of aquatic feeds. *Fish. Sci.* 2002, 68, 242–252.
5. Moon, T. W. Glucose intolerance in teleost fish: fact or fiction? *Comp. Biochem. Physiol. Part B Biochem. Mol. Biol.* 2001, 129, 243–249.
6. HEMRE, G.-I.; MOMMSEN, T. P.; KROGDAHL, A. Carbohydrates in fish nutrition: effects on growth, glucose metabolism and hepatic enzymes. *Aquac. Nutr.* 2002, 8, 175–194.
7. Enes, P.; Panserat, S.; Kaushik, S.; Oliva-Teles, A. Nutritional regulation of hepatic glucose metabolism in fish. *Fish Physiol. Biochem.* 2009, 35, 519–39.
8. Polakof, S.; Panserat, S.; Soengas, J. L.; Moon, T. W. Glucose metabolism in fish: a review. *J. Comp. Physiol. B.* 2012, 182, 1015–45.

9. Li, X. F.; Liu, W. Bin; Lu, K. Le; Xu, W. N.; Wang, Y. Dietary carbohydrate/lipid ratios affect stress, oxidative status and non-specific immune responses of fingerling blunt snout bream, *Megalobrama amblycephala*. *Fish Shellfish Immunol.* 2012, 33, 316–323.
10. Jafri, A. Effect of dietary carbohydrate-to-lipid ratio on growth and body composition of walking catfish (*Clarias batrachus*). *Aquaculture* 1998, 161, 159–168.
11. Lee, S. M.; Kim, K. D.; Lall, S. P. Utilization of glucose, maltose, dextrin and cellulose by juvenile flounder (*Paralichthys olivaceus*). *Aquaculture* 2003, 221, 427–438.
12. TAN, Q.; XIE, S.; ZHU, X.; LEI, W.; YANG, Y. Effect of dietary carbohydrate sources on growth performance and utilization for gibel carp (*Carassius auratus gibelio*) and Chinese longsnout catfish (*Leiocassis longirostris* Gunther). *Aquac. Nutr.* 2006, 12, 61–70.
13. Yasutake, K.; Kohjima, M.; Kotoh, K.; Nakashima, M.; Nakamura, M.; Enjoji, M. Dietary habits and behaviors associated with nonalcoholic fatty liver disease. *World J. Gastroenterol.* 2014, 20, 1756–67.
14. White, J. S. Challenging the fructose hypothesis: new perspectives on fructose consumption and metabolism. *Adv. Nutr.* 2013, 4, 246–56.
15. Rippe, J. M.; Angelopoulos, T. J. Sucrose, high-fructose corn syrup, and fructose, their metabolism and potential health effects: what do we really know? *Adv. Nutr.* 2013, 4, 236–45.
16. Lieschke, G. J.; Currie, P. D. Animal models of human disease: zebrafish swim into view. *Nat. Rev. Genet.* 2007, 8, 353–67.
17. Denechaud, P.-D. et al. Insulin resistance, inflammation, and non-alcoholic fatty liver disease. *Diabetes.* 2013, 27, 371–379.
18. Zhou, Z.; Ren, Z.; Zeng, H.; Yao, B. Apparent digestibility of various feedstuffs for bluntnose black bream *Megalobrama amblycephala* Yih. *Aquac. Nutr.* 2008, 14, 153–165.
19. Li, X.; Liu, W.; Jiang, Y.; Zhu, H.; Ge, X. Effects of dietary protein and lipid levels in practical diets on growth performance and body composition of blunt snout bream (*Megalobrama amblycephala*) fingerlings. *Aquaculture* 2010, 303, 65–70.
20. Brauge, C.; Medale, F.; Corraze, G. Effect of dietary carbohydrate levels on growth, body composition and glycaemia in rainbow trout, *Oncorhynchus mykiss*, reared in seawater. *Aquaculture* 1994, 123, 109–120.
21. Singh, R. K.; Balange, A. K.; Ghughuskar, M. M. Protein sparing effect of carbohydrates in the diet of *Cirrhinus mrigala* (Hamilton, 1822) fry. *Aquaculture* 2006, 258, 680–684.

22. Bou, M.; Todorčević, M.; Fontanillas, R.; Capilla, E.; Gutiérrez, J.; Navarro, I. Adipose tissue and liver metabolic responses to different levels of dietary carbohydrates in gilthead sea bream (*Sparus aurata*). *Comp. Biochem. Physiol. A. Mol. Integr. Physiol.* 2014, 175, 72–81.
23. Zhou, C.; Ge, X.; Niu, J.; Lin, H.; Huang, Z.; Tan, X. Effect of dietary carbohydrate levels on growth performance, body composition, intestinal and hepatic enzyme activities, and growth hormone gene expression of juvenile golden pompano, *Trachinotus ovatus*. *Aquaculture* 2015, 437, 390–397.
24. GAO, W.; LIU, Y.-J.; TIAN, L.-X.; MAI, K.-S.; LIANG, G.-Y.; YANG, H.-J.; HUAI, M.-Y.; LUO, W.-J. Effect of dietary carbohydrate-to-lipid ratios on growth performance, body composition, nutrient utilization and hepatic enzymes activities of herbivorous grass carp (*Ctenopharyngodon idella*). *Aquac. Nutr.* 2009, 16, 327–333.
25. Wilson, R. P. Utilization of dietary carbohydrate by fish. *Aquaculture* 1994, 124, 67–80.
26. Moreira, I. S.; Peres, H.; Couto, A.; Enes, P.; Oliva-Teles, A. Temperature and dietary carbohydrate level effects on performance and metabolic utilisation of diets in European sea bass (*Dicentrarchus labrax*) juveniles. *Aquaculture* 2008, 274, 153–160.
27. Zhou, C.; Ge, X.; Liu, B.; Xie, J.; Chen, R.; Ren, M. Effect of high dietary carbohydrate on the growth performance, blood chemistry, hepatic enzyme activities and growth hormone gene expression of Wuchang bream (*Megalobrama amblycephala*) at two temperatures. *Asian-Australasian J. Anim. Sci.* 2015, 28, 207–214.
28. Zhou, C. P.; Ge, X. P.; Liu, B.; Xie, J.; Miao, L. H. Effect of high dietary carbohydrate on the growth performance and physiological responses of juvenile wuchang bream, *Megalobrama amblycephala*. *Asian-Australasian J. Anim. Sci.* 2013, 26, 1598–1608.
29. Ge, C.-X.; Yu, R.; Xu, M.-X.; Li, P.-Q.; Fan, C.-Y.; Li, J.-M.; Kong, L.-D. Betaine prevented fructose-induced NAFLD by regulating LXR α /PPAR α pathway and alleviating ER stress in rats. *Eur. J. Pharmacol.* 2016, 770, 154–64.
30. Jung, G. Y.; Won, S. B.; Kim, J.; Jeon, S.; Han, A.; Kwon, Y. H. Betaine alleviates hypertriglycemia and tau hyperphosphorylation in db/db mice. *Toxicol. Res.* 2013, 29, 7–14.
31. Kathirvel, E.; Morgan, K.; Nandgiri, G.; Sandoval, B. C.; Caudill, M. A.; Bottiglieri, T.; French, S. W.; Morgan, T. R. Betaine improves nonalcoholic fatty liver and associated hepatic insulin resistance: a potential mechanism for hepatoprotection by betaine. *Am J Physiol Gastrointest Liver Physiol* 2010, 299, 1068–1077.

32. Wang, Z.; Yao, T.; Pini, M.; Zhou, Z.; Fantuzzi, G.; Song, Z. Betaine improved adipose tissue function in mice fed a high-fat diet: a mechanism for hepatoprotective effect of betaine in nonalcoholic fatty liver disease. *Am. J. Physiol. Gastrointest. Liver Physiol.* 2010, 298, G634-42.
33. Wang, L. N.; Liu, W. Bin; Lu, K. Le; Xu, W. N.; Cai, D. Sen; Zhang, C. N.; Qian, Y. Effects of dietary carbohydrate/lipid ratios on non-specific immune responses, oxidative status and liver histology of juvenile yellow catfish *pelteobagrus fulvidraco*. *Aquaculture* 2014, 426–427, 41–48.
34. Kumar, S.; Sahu, N. P.; Pal, A. K.; Choudhury, D.; Yengkokpam, S.; Mukherjee, S. C. Effect of dietary carbohydrate on haematology, respiratory burst activity and histological changes in *L. rohita* juveniles. *Fish Shellfish Immunol.* 2005, 19, 331–44.
35. Mohapatra, M.; Sahu, N. P.; Chaudhari, A. Utilization of gelatinized carbohydrate in diets of *Labeo rohita* fry. *Aquac. Nutr.* 2003, 9, 189–196.
36. Clark, J. M.; Van Natta, M.; Kleiner, D.; Chalasani, N. P.; McCullogh, A. J.; Neuschwander-Tetri, B. A.; Uenalp, A.; Hoofnagle, J. H.; Diehl, A. M. Association of AST and ALT with liver histology in adults with NAFLD. *HEPATOLOGY* 2007, 46, 738A–738A.
37. M-A-Mahtab; Rahman, S.; Karim, F.; Hossain, M. F.; Khan, M. Serum ALT is a better predictor of fibrosis than serum AST in patients with NAFLD: experience from a tertiary centre in Bangladesh. *J. Gastroenterol. Hepatol.* 2008, 23, A45–A46.
38. Waldram, A.; Holmes, E.; Wang, Y.; Rantalainen, M.; Wilson, I. D.; Tuohy, K. M.; McCartney, A. L.; Gibson, G. R.; Nicholson, J. K. Top-Down Systems Biology Modeling of Host Metabotype # Microbiome Associations in Obese Rodents Top-Down Systems Biology Modeling of Host Metabotype - Microbiome Associations in Obese Rodents. 2009, 2361–2375.
39. Lai, Y. S.; Yang, T. C.; Chang, P. Y.; Chang, S. F.; Ho, S. L.; Chen, H. L.; Lu, S. C. Electronegative LDL is linked to high-fat, high-cholesterol diet-induced nonalcoholic steatohepatitis in hamsters. *J. Nutr. Biochem.* 2016, 30, 44–52.
40. Kwon, D. Y.; Jung, Y. S.; Kim, S. J.; Park, H. K.; Park, J. H.; Kim, Y. C. Impaired sulfur-amino acid metabolism and oxidative stress in nonalcoholic fatty liver are alleviated by betaine supplementation in rats. *J. Nutr.* 2009, 139, 63–68.
41. Kharbanda, K. K.; Mailliard, M. E.; Baldwin, C. R.; Sorrell, M. F.; Tuma, D. J. Accumulation of proteins bearing atypical isoaspartyl residues in livers of alcohol-fed rats is prevented by betaine administration: effects on protein-L-isoaspartyl methyltransferase activity. *J. Hepatol.* 2007, 46, 1119–25.

42. Ji, C.; Kaplowitz, N. Betaine decreases hyperhomocysteinemia, endoplasmic reticulum stress, and liver injury in alcohol-fed mice. *Gastroenterology* 2003, 124, 1488–1499.
43. Tang, W.; Zou, J.; Chen, X.; Zheng, J.; Zeng, H.; Liu, Z.; Shi, Y. Association of two polymorphisms within and near SOCS3 gene with obesity in three nationalities in Xinjiang province of China. *Acta Pharmacol. Sin.* 2011, 32, 1381–6.
44. INSR Gene - GeneCards | INSR Protein | INSR Antibody <http://www.genecards.org/cgi-bin/carddisp.pl?gene=INSR> (accessed May 8, 2016).
45. Lynn, F. C. Meta-regulation: microRNA regulation of glucose and lipid metabolism. *Trends Endocrinol. Metab.* 2009, 20, 452–459.
46. Adochio, R. L.; Leitner, J. W.; Gray, K.; Draznin, B.; Cornier, M.-A. Early responses of insulin signaling to high-carbohydrate and high-fat overfeeding. *Nutr. Metab. (Lond)*. 2009, 6, 37.
47. Bayascas, J. R.; Wullschleger, S.; Sakamoto, K.; Garcia-Martinez, J. M.; Clacher, C.; Komander, D.; van Aalten, D. M.; Boini, K. M.; Lang, F.; Lipina, C.; Logie, L.; Sutherland, C.; Chudek, J. A.; van Diepen, J. A.; Voshol, P. J.; Lucocq, J. M.; Alessi, D. R. Mutation of the PDK1 PH domain inhibits protein kinase B/Akt, leading to small size and insulin resistance. *Mol. Cell Biol.* 2008, 28, 3258–3272.
48. Cross, D. A.; Alessi, D. R.; Cohen, P.; Andjelkovich, M.; Hemmings, B. A. Inhibition of glycogen synthase kinase-3 by insulin mediated by protein kinase B. *Nature* 1995, 378, 785–9.
49. Saltiel, A. R.; Kahn, C. R. Insulin signalling and the regulation of glucose and lipid metabolism. *Nature* 2001, 414, 799–806.
50. Hazlehurst, J. M.; Woods, C.; Marjot, T.; Cobbold, J. F.; Tomlinson, J. W. Non-alcoholic fatty liver disease and diabetes. *Metabolism* 2016, 1–13.
51. Zang, M.; Zuccollo, A.; Hou, X.; Nagata, D.; Walsh, K.; Herscovitz, H.; Brecher, P.; Ruderman, N. B.; Cohen, R. A. AMP-activated protein kinase is required for the lipid-lowering effect of metformin in insulin-resistant human HepG2 cells. *J. Biol. Chem.* 2004, 279, 47898–47905.
52. Godlewski, J.; Nowicki, M. O.; Bronisz, A.; Nuovo, G.; Palatini, J.; De Lay, M.; Van Brocklyn, J.; Ostrowski, M. C.; Chiocca, E. A.; Lawler, S. E. MicroRNA-451 Regulates LKB1/AMPK Signaling and Allows Adaptation to Metabolic Stress in Glioma Cells. *Mol. Cell* 2010, 37, 620–632.
53. Diraison, F.; Dusserre, E.; Vidal, H.; Sothier, M.; Beylot, M. Increased hepatic lipogenesis but decreased expression of lipogenic gene in adipose tissue in human obesity. *Am. J. Physiol. Endocrinol. Metab.* 2002, 282, E46–E51.

54. Diraison, F.; Moulin, P.; Beylot, M. Contribution of hepatic de novo lipogenesis and reesterification of plasma non esterified fatty acids to plasma triglyceride synthesis during non-alcoholic fatty liver disease. *Diabetes Metab.* 2003, 29, 478–85.
55. Donnelly, K. L.; Smith, C. I.; Schwarzenberg, S. J.; Jessurun, J.; Boldt, M. D.; Parks, E. J. Sources of fatty acids stored in liver and secreted via lipoproteins in patients with nonalcoholic fatty liver disease. *J. Clin. Invest.* 2005, 115, 1343–51.
56. Hotamisligil, G. S.; Shargill, N. S.; Spiegelman, B. M. Adipose expression of tumor necrosis factor- α : direct role in obesity-linked insulin resistance. *Science* 1993, 259, 87–91.
57. Kern, P. A.; Saghizadeh, M.; Ong, J. M.; Bosch, R. J.; Deem, R.; Simsolo, R. B. The expression of tumor necrosis factor in human adipose tissue. Regulation by obesity, weight loss, and relationship to lipoprotein lipase. *J. Clin. Invest.* 1995, 95, 2111–9.
58. Haukeland, J. W.; Damås, J. K.; Konopski, Z.; Løberg, E. M.; Haaland, T.; Goverud, I.; Torjesen, P. A.; Birkeland, K.; Bjørø, K.; Aukrust, P. Systemic inflammation in nonalcoholic fatty liver disease is characterized by elevated levels of CCL2. *J. Hepatol.* 2006, 44, 1167–74.
59. Dentin, R.; Pégrier, J.-P.; Benhamed, F.; Fougelle, F.; Ferré, P.; Fauveau, V.; Magnuson, M. A.; Girard, J.; Postic, C. Hepatic glucokinase is required for the synergistic action of ChREBP and SREBP-1c on glycolytic and lipogenic gene expression. *J. Biol. Chem.* 2004, 279, 20314–26.
60. Ishii, S.; Iizuka, K.; Miller, B. C.; Uyeda, K. Carbohydrate response element binding protein directly promotes lipogenic enzyme gene transcription. *Proc. Natl. Acad. Sci. U. S. A.* 2004, 101, 15597–602.
61. Ma, L.; Tsatsos, N. G.; Towle, H. C. Direct role of ChREBP.Mlx in regulating hepatic glucose-responsive genes. *J. Biol. Chem.* 2005, 280, 12019–27.
62. Koo, H.-Y.; Wallig, M. A.; Chung, B. H.; Nara, T. Y.; Cho, B. H. S.; Nakamura, M. T. Dietary fructose induces a wide range of genes with distinct shift in carbohydrate and lipid metabolism in fed and fasted rat liver. *Biochim. Biophys. Acta* 2008, 1782, 341–8.
63. Iizuka, K.; Bruick, R. K.; Liang, G.; Horton, J. D.; Uyeda, K. Deficiency of carbohydrate response element-binding protein (ChREBP) reduces lipogenesis as well as glycolysis. *Proc. Natl. Acad. Sci. U. S. A.* 2004, 101, 7281–6.
64. Hasenfuss, S. C.; Bakiri, L.; Thomsen, M. K.; Williams, E. G.; Auwerx, J.; Wagner, E. F. Regulation of steatohepatitis and PPAR α signaling by distinct AP-1 dimers. *Cell Metab.* 2014, 19, 84–95.

65. She, P.; Shiota, M.; Shelton, K. D.; Chalkley, R.; Postic, C.; Magnuson, M. A. Phosphoenolpyruvate carboxykinase is necessary for the integration of hepatic energy metabolism. *Mol. Cell. Biol.* 2000, 20, 6508–17.
66. Hanson, R. W.; Reshef, L. Regulation of phosphoenolpyruvate carboxykinase (GTP) gene expression. *Annu. Rev. Biochem.* 1997, 66, 581–611.
67. Stejskal, E. O.; Tanner, J. E. Spin Diffusion Measurements: Spin Echoes in the Presence of a Time-Dependent Field Gradient. *J. Chem. Phys.* 1965, 42, 288.
68. An, Y.; Xu, W.; Li, H.; Lei, H.; Zhang, L.; Hao, F.; Duan, Y.; Yan, X.; Zhao, Y.; Wu, J.; Wang, Y.; Tang, H. High-fat diet induces dynamic metabolic alterations in multiple biological matrices of rats. *J. Proteome Res.* 2013, 12, 3755–68.
69. Rychlik, W.; Rhoads, R. E. A computer program for choosing optimal oligonucleotides for filter hybridization, sequencing and in vitro amplification of DNA. *Nucleic Acids Res.* 1989, 17, 8543–8551.
70. Luo, W.; Zhang, J.; Wen, J. fu; Liu, H.; Wang, W. min; Gao, Z. xia Molecular cloning and expression analysis of major histocompatibility complex class I, IIA and IIB genes of blunt snout bream (*Megalobrama amblycephala*). *Dev. Comp. Immunol.* 2014, 42, 169–173.
71. Livak, K. J.; Schmittgen, T. D. Analysis of relative gene expression data using real-time quantitative PCR and. *Methods* 2001, 25, 402–408.
72. Tran, N. T.; Gao, Z. X.; Zhao, H. H.; Yi, S. K.; Chen, B. X.; Zhao, Y. H.; Lin, L.; Liu, X. Q.; Wang, W. M. Transcriptome analysis and microsatellite discovery in the blunt snout bream (*Megalobrama amblycephala*) after challenge with *Aeromonas hydrophila*. *Fish Shellfish Immunol.* 2015, 45, 72–82.

Legends

Table 1 Formulation and Proximate compositions of the different experimental diet

Table 2 Growth performance and feed utilization of Blunt Snout Bream (*Megalobrama amblycephala*) fed with control and high carbohydrate diets

Values are mean \pm SEM of three replication. Means in the same line with different superscripts are significantly different ($p < 0.05$). SGR, specific growth rate; FCR, feed conversion ratio; HSI, hepatosomatic index; CF, condition factor.

Table 3 Liver transcriptome profiles in differential expression of Non-alcoholic fatty liver disease (ko04932) and Insulin signaling pathway (ko04910) genes by blunt snout bream from comparative of control and HCBD group

Figure 1 Representative hematoxylin and eosin- stained histological section of fish liver. (A) Blunt snout bream fed with normal dietary and (B) fed with high carbohydrate dietary.

Noted: Represent arrow (A) Normal hepatic cell, (B) Swelling hepatocytes with diffuse and large of lipid vacuolization, (C) absent nucleus and (D) abnormal nucleus.

Figure 2 Blood biochemical parameters.

Results were analyzed by t-test. (*) above bar indicated significant differences ($P < 0.05$), (**) above bar indicated highly significant differences ($P < 0.01$).

Figure 3 The metabolites changed in the plasma and liver extracts between control and HCBD diet. (A) Plasma metabolomics and (B) Liver betaine metabolomics

Results were analyzed by t-test. (*) above bar indicated significant differences ($P < 0.05$), (**) above bar indicated highly significant differences ($P < 0.01$).

Figure 4 The transcriptome profiles analysis between control and HCBD group. (A) COG annotation, (B) GO annotation, (C) The difference expression by MA plot and (D) The KEGG annotation

Figure 5 The difference gene expression of mRNA in liver of blunt snout bream when fed with high carbohydrate diet by qRT-PCR. Data were normalized to 18s rRNA and Rp113a as a reference gene and presented as a fold change between control and HCBD group (mean \pm SE), Results were analyzed by t-test. (*) above bar indicated significant differences ($P < 0.05$), (**) above bar indicated highly significant differences ($P < 0.01$)

Figure 6 The change of transcriptome, serum and liver metabolomics and serum biochemistry by high carbohydrate diet lead to fatty liver disease

Table 1

<i>Ingredient</i>	<i>Experimental diet (%)</i>	
	Control	HCBD
Soy bean meal	35.50	34.00
Rapeseed meal	19.00	19.00
Wheat bran	1.20	1.20
Fish meal	8.00	8.00
Flour	18.00	26.30
Soy bean oil	3.80	5.20
Lys	0.30	0.30
Ca(H ₂ PO ₄)	2.00	2.00
Premix	1.00	1.00
Choline chloride	1.00	1.00
Carboxymethyl cellulose	2.00	2.00
Bentonite	8.20	0.00
<i>Proximate compositions (%)</i>		
Protein	30.84	30.28
Lipid	7.99	8.26
Carbohydrate	26.63	34.13
Energy	17.00	17.00

Table 2

Item	Treatment	
	Control	HCBD
Survival rate (%)	94.82±7.14 ^a	97.78±2.22 ^a
Initial weight (g)	48.15±0.55 ^a	48.11±0.22 ^a
Final weight (g)	65.28±2.95 ^a	68.53±2.78 ^a
Weight gain (%)	35.56±5.14 ^a	42.42±5.13 ^a
SGR (%day ⁻¹)	0.51±0.06 ^a	0.59±0.06 ^a
FCR	2.68±0.27 ^a	2.45±0.14 ^a
HSI (%)	1.40±0.14 ^a	1.52±0.13 ^b
CF (%)	2.06±0.10 ^a	2.03±0.11 ^a

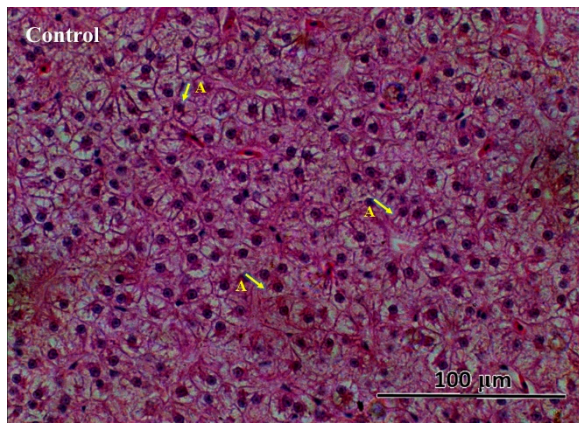
Table 3

Gene Name	KEGG Number	Nr_annotation	FDR	log2FC	Up-Down
SOCS3 ¹²	K04696	Suppressor of cytokine signaling 3b [Danio rerio]	0.009144	-2.802	down
INSR ¹²	K04527	Insulin receptor a precursor [Danio rerio]	0.272547	1.070	up
IRS ¹²	K07187	Insulin receptor substrate 2-B-like [Danio rerio]	0.013461	1.903	up
PI3K ¹²	K02649	Phosphatidylinositol 3-kinase regulatory subunit beta, partial [Anas platyrhynchos]	0.048268	-5.230	down
PDK1 ²⁴	K06276	3-phosphoinositide-dependent protein kinase 1 isoform X1 [Danio rerio]	0.050913	1.603	up
Akt ¹²	K04456	RAC-gamma serine/threonine-protein kinase [Danio rerio]	0.000433	6.580	up
GSK3 ¹²	K03083	Glycogen synthase kinase-3 beta-like [Lepisosteus oculatus]	3.08E-13	-8.657	down
	K03083	Glycogen synthase kinase-3 beta-like isoform X3 [Neolamprologus brichardi]	0.002352	-6.405	down
AMPK ¹²	K07198	MAP/microtubule affinity-regulating kinase 3 [Danio rerio]	8.08E-13	-8.608	down
	K07198	MAP/microtubule affinity-regulating kinase 3 [Esox lucius]	0.038900	-5.459	down
	K07198	Serine/threonine-protein kinase MARK1-like [Stegastes partitus]	0.012837	-5.540	down
ACC ²	K11262	Acetyl-CoA carboxylase 2 isoform X2 [Danio rerio]	1	0.369	up
AP-1 ¹	K04448	Transcription factor AP-1 [Oncorhynchus mykiss]	5.72E-05	6.614	up
PEPCK ²	K01596	Phosphoenolpyruvate carboxykinase [Acanthopagrus schlegelii]	0.002169	5.994	up
FBP ²	K03841	Fructose-1,6-bisphosphatase 1-like [Xiphophorus maculatus]	0.007951	6.039	up
	K03841	Fructose-1,6-bisphosphatase 1-like isoform X3 [Cynoglossus semilaevis]	0.007492	6.142	up
	K03841	Fructose-1,6-bisphosphatase 1-like [Poecilia reticulata]	1.95E-10	-8.129	down
	K03841	Fructose-1,6-bisphosphatase 1-like [Oryzias latipes]	0.020039	-5.485	down
	K03841	Fructose-1,6-bisphosphatase 1-like [Poecilia formosa]	0.040649	-5.577	down

Noted: ¹Non-alcoholic fatty liver disease pathway (ko04932), ²Insulin signaling pathway (ko04910)

Figure 1

(A)



(B)

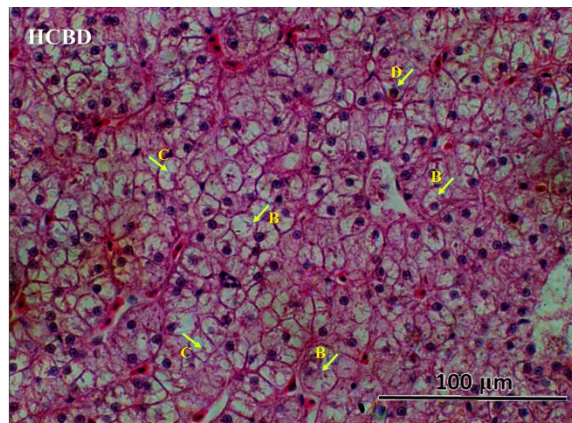


Figure 2

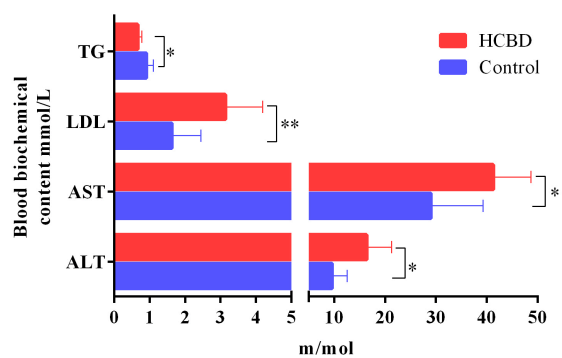
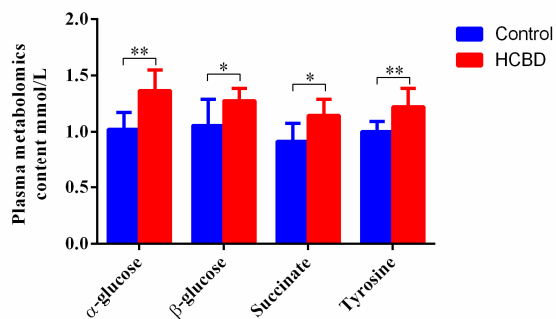


Figure 3

(A)



(B)

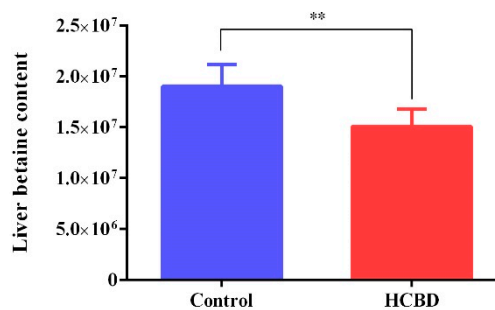
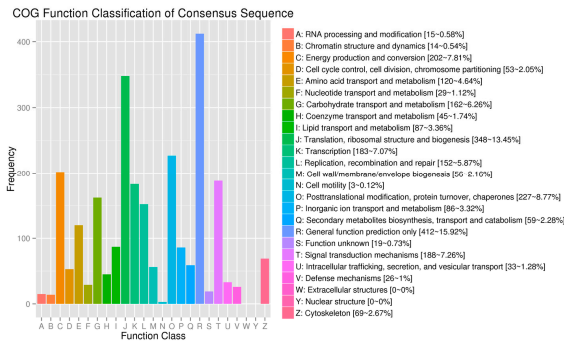
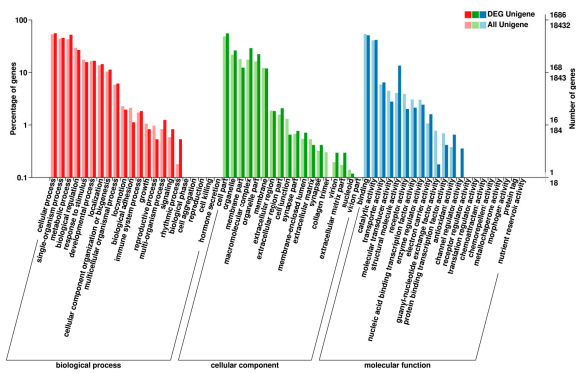


Figure 4

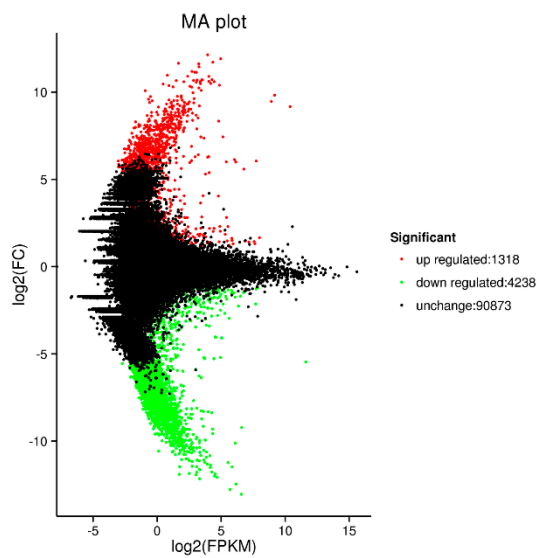
(A)



(B)



(C)



(D)

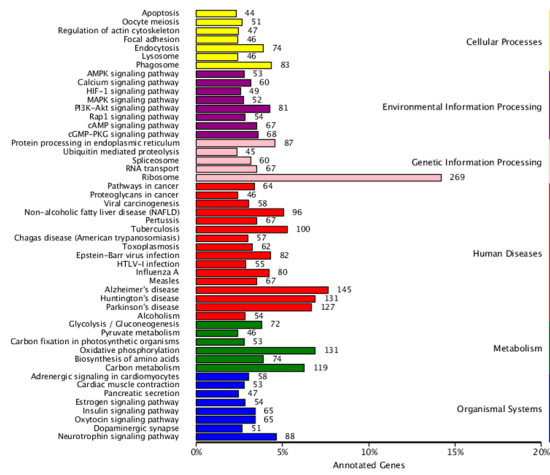


Figure 5

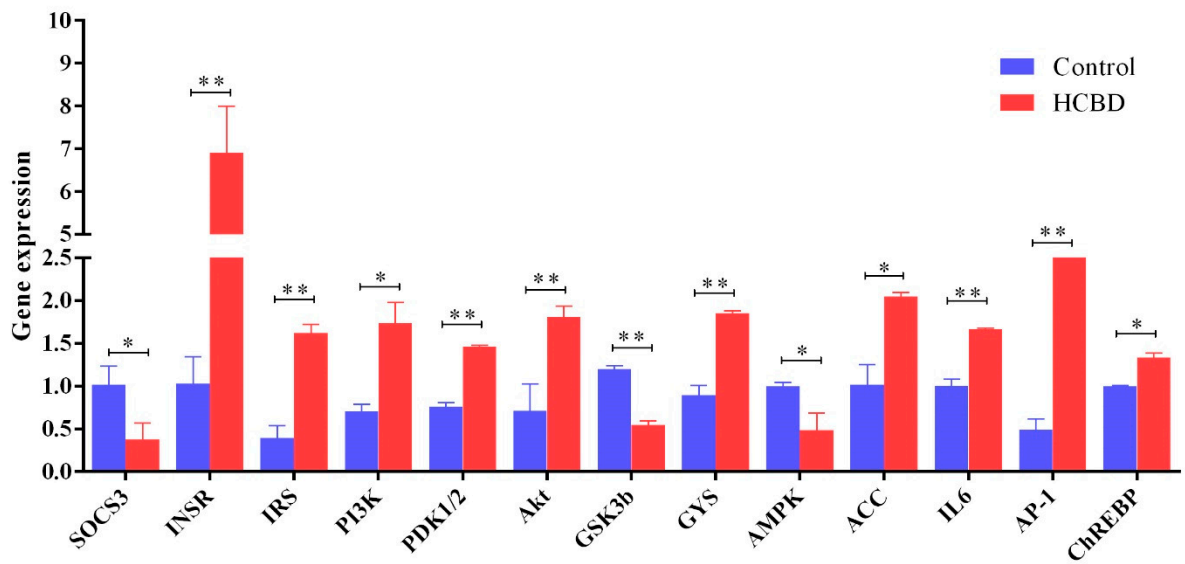
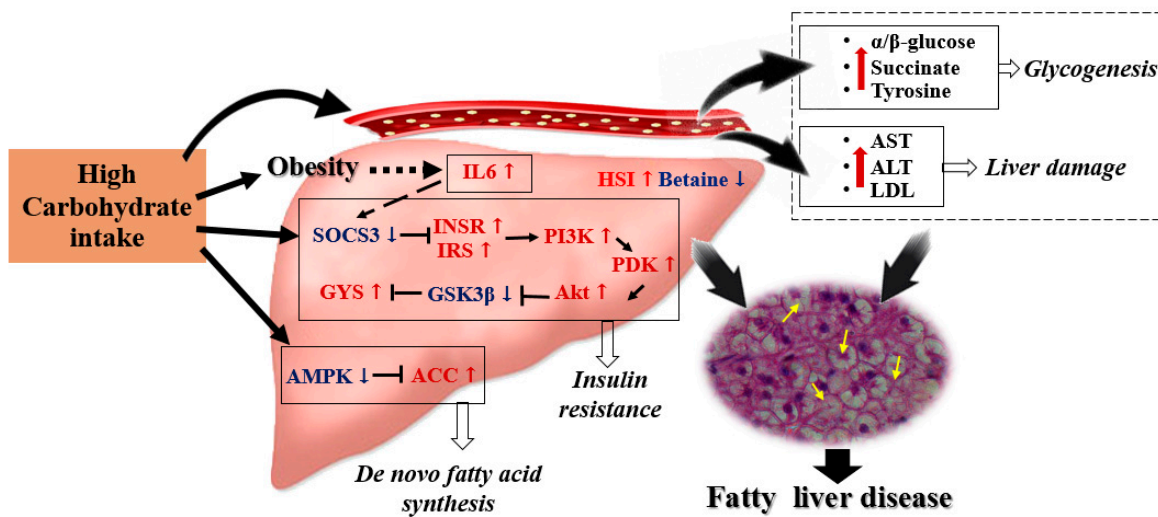
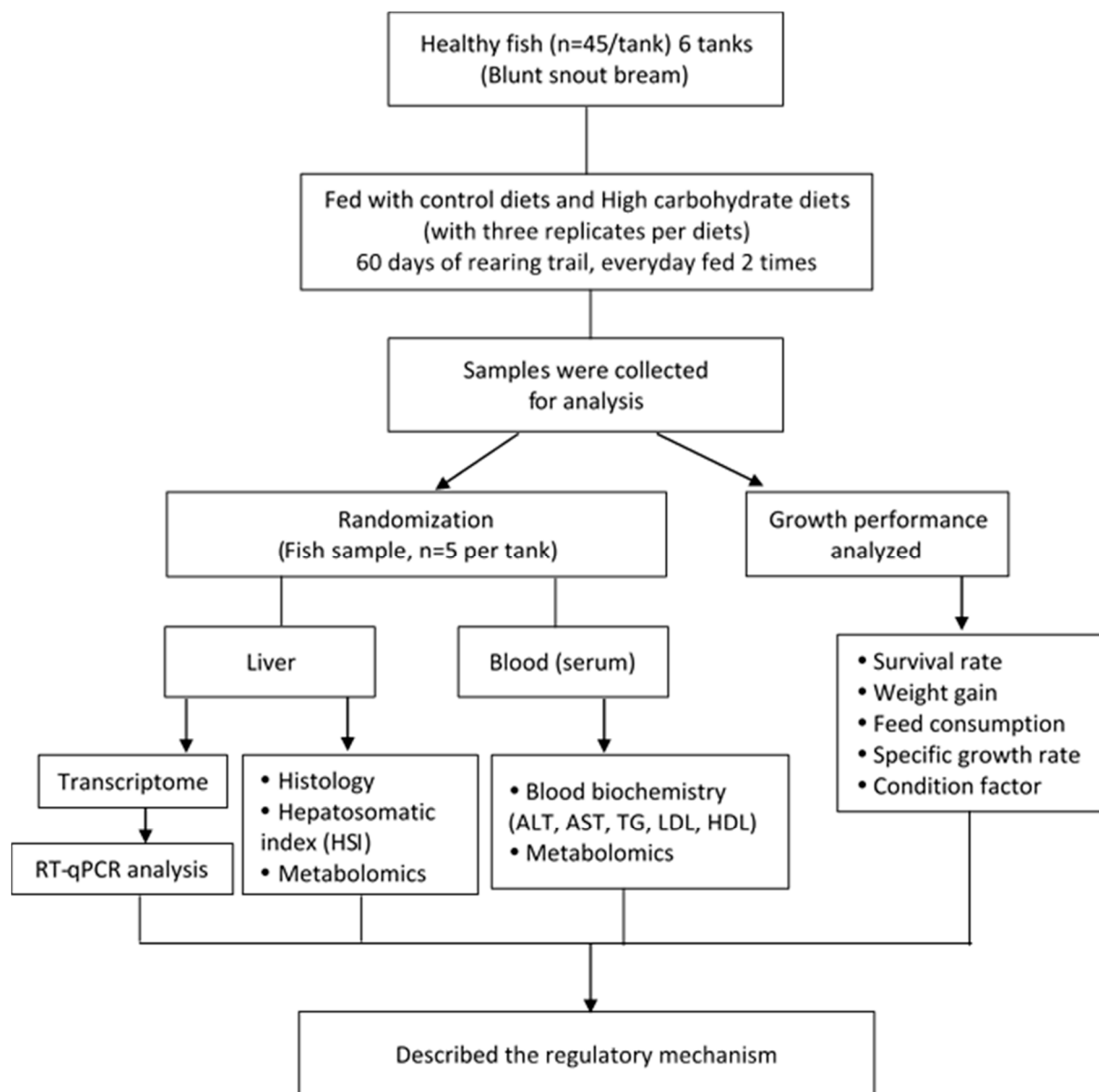


Figure 6



Study designs diagram



© 2017 by the authors; licensee *Preprints*, Basel, Switzerland. This article is an open access article distributed under the terms and conditions of the Creative Commons by Attribution (CC-BY) license (<http://creativecommons.org/licenses/by/4.0/>).